WELL-POSED BOUNDARY CONDITIONS FOR SEMI-LAGRANGIAN SCHEMES; THE ONE-DIMENSIONAL CASE.

A McDonald
Met Éireann
Dublin, Ireland.

1. INTRODUCTION

In a limited area model the lateral borders are not physical boundaries to the flow but, instead, artificial constructs imposed by our desire to model what is happening in a sub-volume of the global atmosphere. In order to solve the equations describing the evolution of the atmosphere in that sub-volume we must supply values for the fields at these artificial boundaries. Doing this correctly is a rather subtle matter. As Oliger and Sundström (1978) have shown, for each inward pointing characteristic a field must be supplied at the lateral boundary. This implies that only a certain sub-set of all the variables should be imposed. If this sub-set has been correctly chosen then we will say the problem is 'well-posed'; if not, 'ill-posed'.

Constructing a well-posed system is a daunting task. For that reason, and because an easy-to-implement alternative solution to the boundary problem exists, numerical weather prediction models with well-posed lateral boundaries have never got farther than the 'drawing-board' stage of existence; see, for example, Elvius and Sundström (1973). That alternative is to over-specify the boundaries and damp the resulting noise with a relaxation scheme; see Davies(1976). This gives stable forecasts and is almost trivial to implement. Evidence of its success is its almost universal use in operational limited area numerical weather prediction models. It is also used in many research models.

Despite this there are a number of reasons for taking a fresh look at well-posed boundaries. (i) There is evidence that the flow relaxation scheme can cause mass loss or gain; see McDonald (1998). (ii) At points at which the characteristic velocity is pointing out of the domain of integration *we are imposing the external model solution when we do not need to* if we use the flow relaxation scheme. Thus we may introduce *unnecessary* errors when these fields are incorrect (as they must be in an operational environment). (iii) In

the near future 4d-var will be used in the forecast-analysis cycle. This has implications for our boundary treatment. Because of the iterative nature of 4d-var the influence of the boundary conditions spreads farther into the limited area domain with each iteration. When the adjoint model is integrated backward in time, what were formerly boundary points with incoming characteristic velocities may become points describing error gradient fields with outgoing characteristic velocities. These must now pass out of the limited area without reflection . 'Over-specify and relax' may not be sufficiently subtle to accommodate these requirements. If our boundary treatment is only partially successful in doing this then one may speculate that this error could build on itself as we continue the forecast-analysis cycle. See Gustafsson, Källén, and Thorsteinsson (1998). (iv) A theoretical development has occurred which makes the practical implementation of well-posed boundaries for numerical weather prediction much more feasible. Engquist and Majda (1977) have shown how to reduce false wave reflection at the boundaries to a minimum while maintaining well-posedness.

For these reasons the HIRLAM group has decided to make a serious attempt at building a numerical weather prediction model which has well-posed boundaries. This report takes a first step in that direction by looking at the technical problems encountered in solving the one-dimensional advection and one-dimensional advection-adjustment equations with well-posed boundaries when using semi-Lagrangian and semi-implicit (SLSI) discretization on an Arakawa C-grid. Examining the one-dimensional advection equation (see section 2) allows us to ask the question: how do we maintain well-posedness when the departure point is outside the integration area, in isolation from the complications introduced by the C-grid and the semi-implicit scheme. These latter complications are considered in section 3. Finally, a discussion of some of the points raised and what the next step should be is included in section 4.

2. THE ONE DIMENSIONAL ADVECTION EQUATION.

The one-dimensional advection equation is ideal for looking at the semi-Lagrangian discretization in isolation. Well-posedness is transparent, and complications introduced by the C-grid, the semi-implicit scheme, and higher spatial dimensions are absent. Therefore let us start with it:

$$\frac{\partial \phi(x,t)}{\partial t} + \bar{u}\frac{\partial \phi(x,t)}{\partial x} = 0, \tag{2.1}$$

where $0 \leq x \leq L, t > 0$, and $\bar{u}$ is a constant velocity. An initial condition is needed: $\phi(x,0) = f(x)$. Also, a boundary condition is needed: $\phi(0,t) = g(t)$, if $\bar{u} > 0$. If $\bar{u} < 0$ the boundary condition must be supplied at L.

If the solution enters through the boundary at $x = 0$ and exits through the boundary at $x = L$ without distortion or reflection the *discretization* is well-posed. For that discretization let us use the semi-Lagrangian scheme. The solution to Eq. (2.1) is

$$\phi_i^{n+1} = \phi(i\Delta x - \bar{u}\Delta t, n\Delta t) = \phi_*^n, \tag{2.2}$$

where $\phi_i^n = \phi(i\Delta x, n\Delta t)$. The arrival point is at $i\Delta x$ and the departure point, x_*, is at $i\Delta x - \bar{u}\Delta t$. With a Lagrange cubic interpolation,

$$\phi_*^n = -\frac{1}{6}\hat{\alpha}(1-\hat{\alpha})(2-\hat{\alpha})\phi_{i-p+1}^n + \frac{1}{2}(1-\hat{\alpha})(1+\hat{\alpha})(2-\hat{\alpha})\phi_{i-p}^n$$

$$+\frac{1}{2}\hat{\alpha}(1+\hat{\alpha})(2-\hat{\alpha})\phi_{i-p-1}^n - \frac{1}{6}\hat{\alpha}(1-\hat{\alpha})(1+\hat{\alpha})\phi_{i-p-2}^n, \qquad (2.3)$$

where $\alpha = \bar{u}\Delta t/\Delta x$; $p = [\alpha]$ if $\alpha \geq 0$ and $p = [\alpha - 1]$ if $\alpha < 0$; $[\alpha]$ is the integer part of α; $p + \hat{\alpha} = \alpha$. To maintain stability p must be chosen such that $(i-p-1)\Delta x \leq x_* \leq (i-p)\Delta x$ or equivalently $0 \leq \hat{\alpha} \leq 1$. See Bates and McDonald (1982), for more details.

If the departure point is outside the area we cannot use Eq. (2.3). We examine various methods for addressing this problem below. Nor can we use Eq. (2.3) when the departure point lies in the grid box immediately next to the boundary. In that case let us use a Lagrange quadratic interpolation:

$$\phi_*^n = -\frac{1}{2}\hat{\alpha}(1-\hat{\alpha})\phi_{i-p+1}^n + (1+\hat{\alpha})(1-\hat{\alpha})\phi_{i-p}^n + \frac{1}{2}(1+\hat{\alpha})\hat{\alpha}\phi_{i-p-1}^n \qquad (2.4a)$$

when $0 \leq x_* < \Delta x$ and

$$\phi_*^n = \frac{1}{2}(1-\hat{\alpha})(2-\hat{\alpha})\phi_{i-p}^n + \hat{\alpha}(2-\hat{\alpha})\phi_{i-p-1}^n - \frac{1}{2}\hat{\alpha}(1-\hat{\alpha})\phi_{i-p-2}^n \qquad (2.4b)$$

when $L - \Delta x \leq x_* < L$.

Let us consider the outflow boundary first. Recall that for well-posedness we *must not impose* a value of ϕ at this boundary; we must extrapolate from the interior. The semi-Lagrangian scheme provides us with an ideal way of doing this. When $|\alpha| < 1$; then we use Eq. (2.4). It yields an $O(\Delta x^2)$ accurate solution. If $|\alpha| \geq 1$ then we use Eq. (2.3), which is $O(\Delta x^3)$ accurate.

It is interesting to note that if, for example, we were using the leapfrog scheme to integrate Eq. (2.1) we would have to switch to either Eq. (2.4) or some other upwind type of discretization in order to compute ϕ at the outflow boundary point. See McDonald (1997), for example.

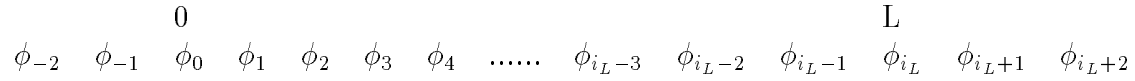

FIGURE 2.1. Distribution of variables on the x-axis.

Next consider the inflow boundary and points in its immediate vicinity. On the boundary line itself we must *impose* a value on the field. If $|\alpha| > 1$ then updating ϕ at the grid points adjacent to the inflow boundary causes difficulties. We return to this below. If

$|\alpha| \leq 1$, then $p = 0$, we can proceed as follows. Assuming $\bar{u} > 0$, we *impose* ϕ_0^{n+1}. We compute ϕ_1^{n+1} using Eq. (2.4a). Over the range $i = 2 \rightarrow i_L - 1$, we use Eq. (2.3), and for $\phi_{i_L}^{n+1}$ we use Eq. (2.4b); ($x_{i_L} = L$; see figure 2.1).

To test this let us model a 'bell curve' of 'width' $L/10$ being advected in the positive direction along the x-axis with a velocity $\bar{u}$, starting with the maximum of the bell curve at $x = x_s$. At any subsequent time t the position of that maximum will be at $x(t) = x_s + \bar{u}t$. The initial condition is

$$\phi(x, 0) = \hat{\phi} exp[-\{(x - x_s)/(L/10)\}^2] \ . \tag{2.5}$$

Consider $\bar{u} > 0$ without loss of generality. Then we must supply a boundary condition at $x = 0$:

$$\phi(0, t) = \hat{\phi} exp[-\{(0 - x(t))/(L/10)\}^2]; \qquad t > 0. \tag{2.6}$$

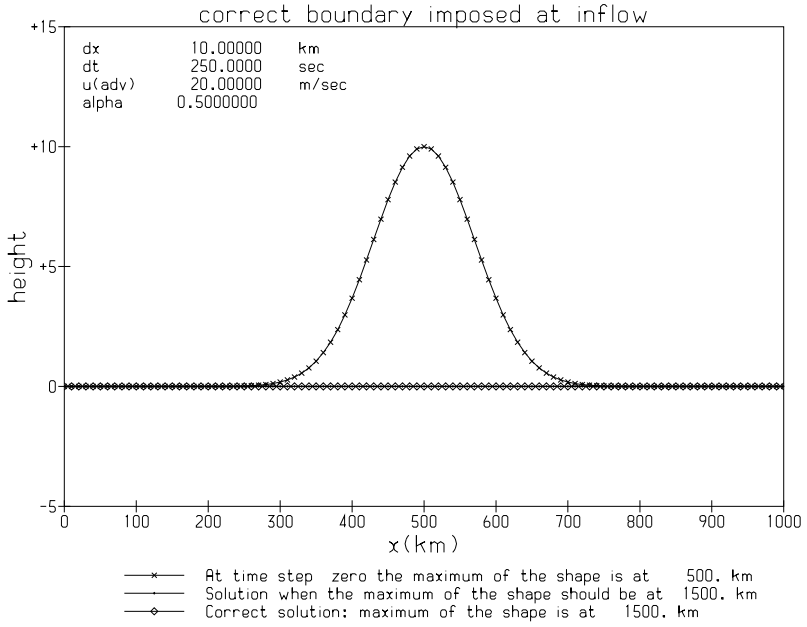

FIGURE 2.2. Graph of the solution for test 1. At time zero the bell curve, centered at 500km, is shown by the 'x's. The analytical solution, which has it centered at 1500km, is represented by the diamonds. The result of integrating with $\alpha = 0.5$ is shown by the dots.

The following parameters will be used in the tests of our discretization. $\Delta x = 10$km, $\bar{u} = 20$m/s , $L = 1000$km, $\hat{\phi} = 10$. We will perform the following two experiments.

Test 1 : start with the bell-curve centered at $x = L/2$ and choose the time such that at the end of the integration it will be centered at $3L/2$ in order to see whether it passes through the boundary at $x = L$ without false reflections.

Test 2: start with the bell-curve centered at $x = -L/2$ and choose the time such that at the end of the integration it will be centered at $L/2$ in order to see whether it passes through the boundary at $x = 0$ without distortion.

With $\alpha = 0.5$ it passes both tests. Figure 2.2 shows the result of *test 1*. The bell curve has exited through the boundary accurately. There are no false reflections (the dots coincide exactly with the diamonds). Figure 2.3 shows the result of *test 2*. The bell curve has entered the area accurately (the dots coincide almost exactly with the diamonds).

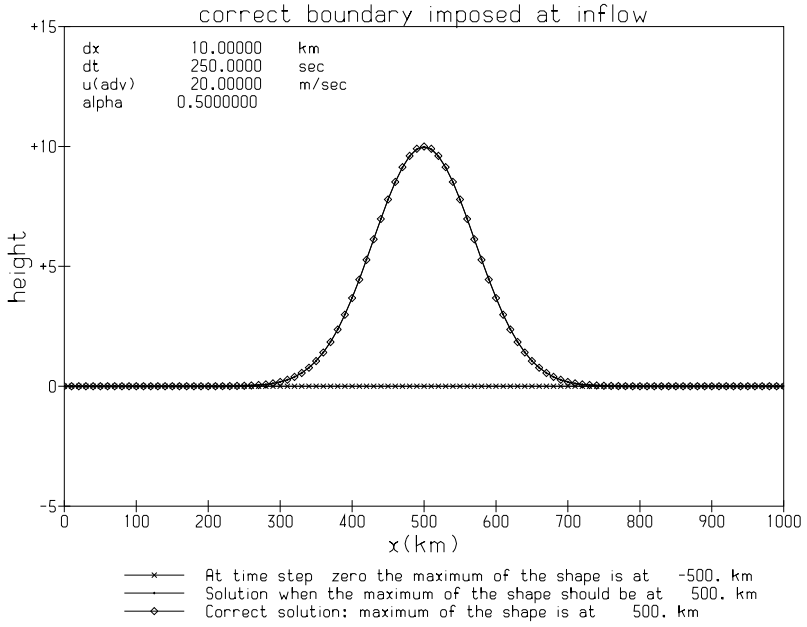

FIGURE 2.3. Graph of the solution for test 2. At time zero the bell curve, centered at -500km, is shown by the 'x's. The analytical solution which has it centered at 500km is represented by the diamonds. The result of integrating with $\alpha = 0.5$ *is shown by the dots.*

Let us return to the problem near the inflow boundary when $|\alpha| > 1$. We now have $|p| > 0$, and when, for example, $\bar{u} > 0$, the departure point associated with ϕ_1 is outside the area. What are the options?

Option 1; trajectory truncation. If the departure point is beyond the boundary, then truncate the trajectory at the boundary. Thus, for example, if the departure point associated with ϕ_2 were at $x = -\Delta x/2$ we would use for Eq. (2.2):

$$\phi_2^{n+1} = \phi^n(-\Delta x/2, n\Delta t) \approx \phi^n(0, n\Delta t). \tag{2.7}$$

This method is stable but slightly inaccurate, as can be seen from figure 2.4, which shows the result of repeating *test 2* with $\alpha = 2.5$

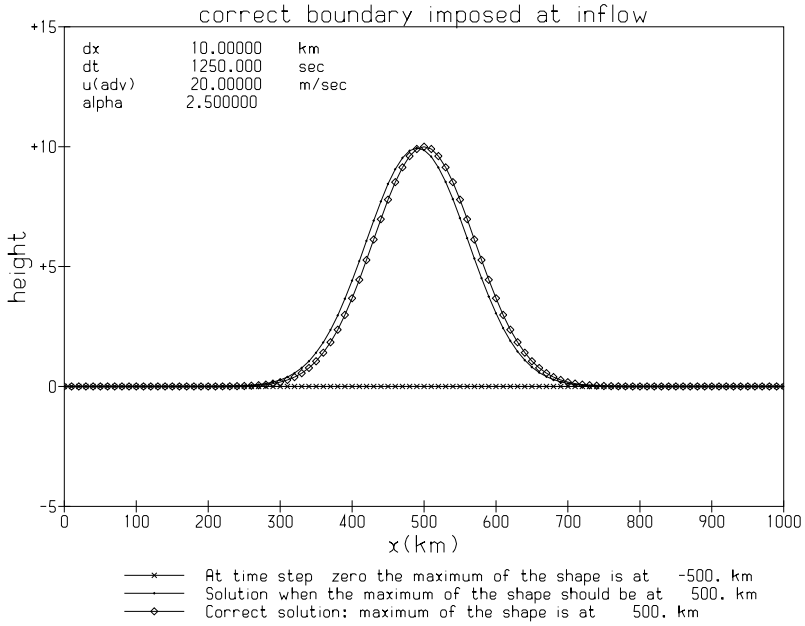

FIGURE 2.4. Same as figure 2.3, but using the trajectory truncation scheme (option 1) and $\alpha = 2.5$

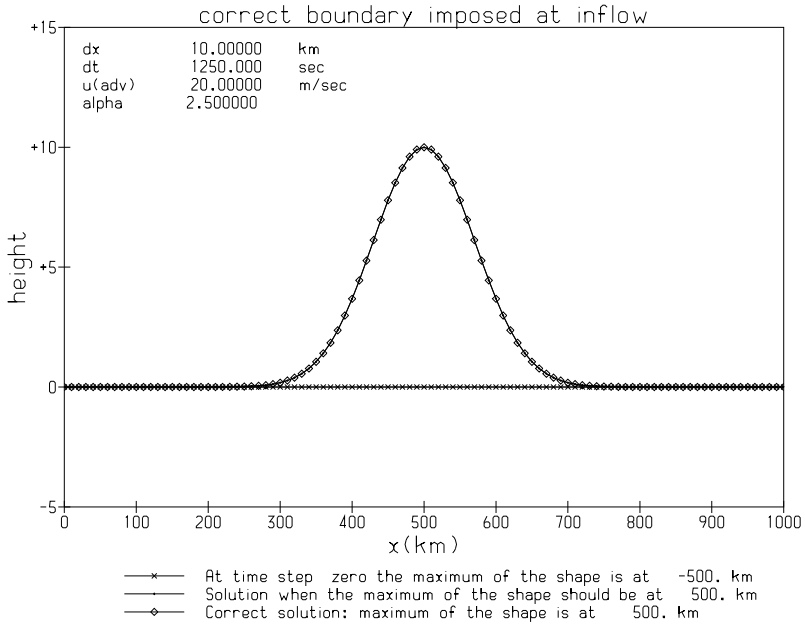

FIGURE 2.5. Same as figure 2.3, but using the externally sourced buffer zone (option 2) and $\alpha = 2.5$.

Option 2; externally sourced buffer zone. Add a buffer zone outside the inflow boundary line in which the fields are also supplied from an external source. Use these fields to

interpolate to the departure point. Looked at from a Lagrangian point of view this seems a very natural thing to do; this is where the parcels are coming from. However, looking at it from an Eulerian point of view we see that we no longer have a classic initial-boundary value problem.

Nevertheless, let us repeat *test 2* with $\alpha = 2.5$. The result is that full accuracy is restored. See figure 2.5.

Option 3; time interpolation. Let us try to improve the accuracy of the trajectory truncation method. Recall that at inflow we know the field value at every time step on the boundary line, in principle, anyway. Let us use this information by invoking an idea of Skålin and Lie (1995). See also Falcone and Ferretti (1998).

Consider the following argument. The solution to Eq. (2.1) can be written as

$$\phi(x_i, t + \delta t) = \phi(x_i - \bar{u}\delta t, t) \tag{2.8}$$

Choose $\bar{u}\delta t = \mu\Delta x$, where μ is a non-zero integer. Also choose $t + \delta t = (n + 1)\Delta t$. Substituting in Eq. (2.8) we get

$$\phi\{x_i, (n + 1)\Delta t\} = \phi\{x_{i-\mu}, (n + 1 - \frac{\mu}{\alpha})\Delta t\} \tag{2.9}$$

For the following argument consider $\bar{u} > 0$. There is no loss of generality. Let $i = \mu$; then this equation expresses the value of the field at time $(n + 1)\Delta t$ at the interior grid point, μ, in terms of the field on the boundary line, $i = 0$, at time $(n + 1 - \mu/\alpha)\Delta t$. The field is not known at this time. However, we can 'interpolate in time' because, in principle, on the boundary line we know $\phi\{x_0, m\Delta t\}$ for all integer $m > 0$. For example, using a Lagrange linear interpolation for the right hand side of Eq. (2.9) yields

$$\phi_\mu^{n+1} = (1 - \frac{\mu}{\alpha})\phi_0^{n+1} + \frac{\mu}{\alpha}\phi_0^n \tag{2.10}$$

This is stable from a von Neumann point of view, anyway, because $0 < \mu/\alpha < 1$. When $|\alpha| < \mu$ we do not use this approach to finding the departure point value of the field; we use Eq. (2.4). The easiest way to see this is to draw a picture; see figure 2.6, which illustrates the situation when $\alpha = 2.5$. When we compute ϕ_1^{n+1} we solve Eq. (2.10) with $\mu = 1$. The traditional departure point is at 'E' in figure 2.6, but now we use the known values of ϕ_0 at 'A' and 'F' to interpolate ϕ_0 to the point 'H'. Simple geometry shows 'AH/AF' $= 1/\alpha < 1$. When we compute ϕ_2^{n+1} we solve Eq. (2.10) with $\mu = 2$. We use the values of ϕ_0 at 'A' and 'F' to interpolate ϕ_0 to the point 'G'. Again, simple geometry shows 'AG/AF' $= 2/\alpha < 1$. When we compute ϕ_3^{n+1} the traditional departure point is at 'K', and we return to interpolating in space, using Eq. (2.4) to find the departure point value.

We can generalise. The line 'AF' will be cut by $\mu = [\alpha]$ trajectories, where $[\alpha]$ is the integer part of α. Thus $\mu/\alpha < 1$.

If, instead, we have inflow at the $x = L$ boundary we choose $i = \mu + i_L$. Both μ and α are now negative but the arguments are the same and instead of Eq. (2.10) we use

$$\phi^{n+1}_{\mu+i_L} = (1 - \frac{\mu}{\alpha})\phi^{n+1}_{i_L} + \frac{\mu}{\alpha}\phi^{n}_{i_L}. \tag{2.11}$$

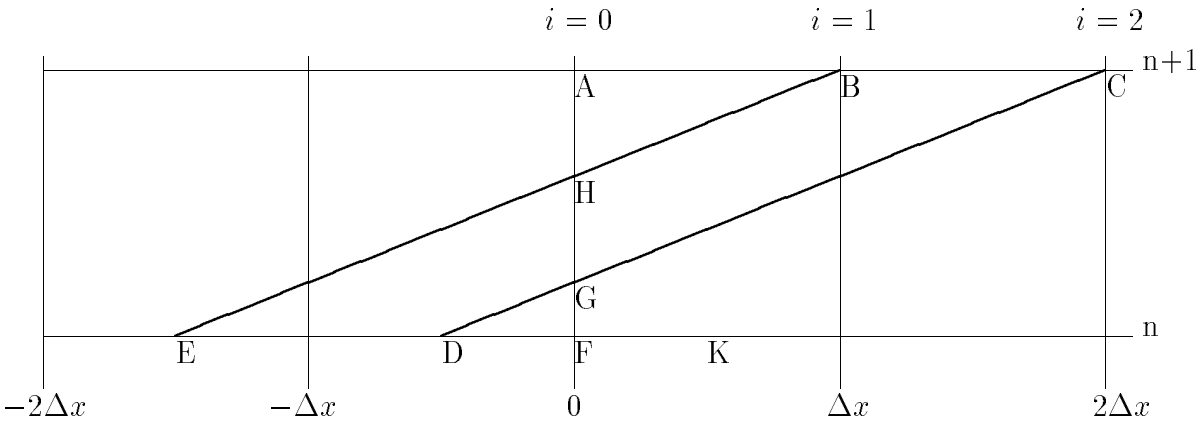

FIGURE 2.6. Space-time diagram centered on the boundary line at $x = 0$; $\alpha = 2.5$.

Obviously, $O(\Delta t^2)$ accuracy can be achieved by using a Lagrange quadratic interpolation,

$$\phi^{n+1}_i = C_+\left(\frac{\mu}{\alpha}\right)\phi^{n+1}_{i-\mu} + C_0\left(\frac{\mu}{\alpha}\right)\phi^{n}_{i-\mu} + C_-\left(\frac{\mu}{\alpha}\right)\phi^{n-1}_{i-\mu}, \tag{2.12}$$

where

$$C_+\left(\frac{\mu}{\alpha}\right) = \frac{1}{2}(1 - \frac{\mu}{\alpha})(2 - \frac{\mu}{\alpha}); \quad C_0\left(\frac{\mu}{\alpha}\right) = \frac{\mu}{\alpha}(2 - \frac{\mu}{\alpha}); \quad C_-\left(\frac{\mu}{\alpha}\right) = -\frac{1}{2}\frac{\mu}{\alpha}(1 - \frac{\mu}{\alpha}) \tag{2.13}$$

instead of Eqs. (2.10) and (2.11). I have used the linear scheme above in order to prevent any messy algebra from obscuring the ideas under discussion.

I repeated *test 2* with $\alpha = 2.5$, using quadratic interpolation in time at the inflow boundary. Full accuracy is restored. The figure (not shown) looks identical to figure 2.5.

Option 4; well-posed buffer zone. Let us return to the idea of having a buffer zone and try to make it well-posed. Instead of supplying the field values in the buffer zone from an external source let us compute them using only information from the inflow boundary line. Again, for the purpose of demonstration consider the situation when $\bar{u} > 0$. Then we wish to compute ϕ_{-1}, ϕ_{-2}, etc., in figure 2.1.

Naive extrapolation from the interior to the inflow boundary will cause instability. Thus we cannot, for example, use Eq. (2.3) to extrapolate, abandoning the restriction $0 < \hat{\alpha} \leq 1$. (A von Neumann stability analysis shows that for $\hat{\alpha} = -2$ the amplification factor is 15 for the two-grid wave; see Eq. (23) of McDonald (1984)).

Since for well-posedness we must supply $\phi(0,t)$ for all t we know $\partial\phi(0,t)/\partial t, \partial^2\phi(0,t)/\partial t^2$, and so on. Thus, from Eq. (2.1) we know

$$\frac{\partial\phi(0,t)}{\partial x} = -\frac{1}{\bar{u}}\frac{\partial\phi(0,t)}{\partial t} \quad , \frac{\partial^2\phi(0,t)}{\partial x^2} = \frac{1}{\bar{u}^2}\frac{\partial^2\phi(0,t)}{\partial t^2}, \tag{2.14}$$

and so on, enabling us to estimate ϕ_{-1}, ϕ_{-2}, etc. using a Taylor expansion:

$$\phi(-i\Delta x,t) = \left[\phi - i\Delta x\frac{\partial\phi}{\partial x} + \frac{(i\Delta x)^2}{2}\frac{\partial^2\phi}{\partial x^2} + ...\right]_0^t \tag{2.15}$$

When $\bar{u} < 0$ the same procedure can be used to compute $\phi(L + i\Delta x)$.

I repeated *test 2* with $\alpha = 2.5$, using this procedure to compute the necessary fields in the boundary zone. Full accuracy is restored. The figure (not shown) looks identical to figure 2.5.

3. THE ONE DIMENSIONAL ADVECTION-ADJUSTMENT EQUATION.

In this section we add in 'adjustment' in its simplest form in order to explore the following complications which arise when using the two time level SLSI discretization. (a) What difficulties are caused by using the C-grid? (b) How do we maintain well-posedness when choosing the boundary conditions for the Helmholtz equation generated by the semi-implicit scheme. (c) How do we maintain well-posedness when the departure point is outside the area of integration?

Thus, let us solve the one-dimensional shallow water equations

$$\frac{\partial\phi(x,t)}{\partial t} + \bar{u}\frac{\partial\phi(x,t)}{\partial x} + \bar{\phi}\frac{\partial u(x,t)}{\partial x} = 0, \tag{3.1}$$

$$\frac{\partial u(x,t)}{\partial t} + \bar{u}\frac{\partial u(x,t)}{\partial x} + \frac{\partial\phi(x,t)}{\partial x} = 0, \tag{3.2}$$

where $\bar{u}$ and $\bar{\phi}$ are constants. It is easy to show that the following ϕ and u satisfy Eqs. (3.1) and (3.2):

$$\phi(x,t) = Aexp[i\frac{2\pi}{L_x}\{x - (\bar{u}+\bar{c})t\}] + Bexp[i\frac{2\pi}{L_x}\{x - (\bar{u}-\bar{c})t\}] \tag{3.3}$$

$$u(x,t) = \frac{A}{\bar{c}}exp[i\frac{2\pi}{L_x}\{x - (\bar{u}+\bar{c})t\}] - \frac{B}{\bar{c}}exp[i\frac{2\pi}{L_x}\{x - (\bar{u}-\bar{c})t\}]. \tag{3.4}$$

A and B are constants; L_x is the wavelength, and $\bar{c} = \sqrt{\bar{\phi}}$. By re-arranging Eqs. (3.1) and (3.2) as

$$\left[\frac{\partial}{\partial t} + (\bar{u}+\bar{c})\frac{\partial}{\partial x}\right]\left[u + \frac{\phi}{\bar{c}}\right] = 0, \tag{3.5}$$

$$\left[\frac{\partial}{\partial t} + (\bar{u} - \bar{c})\frac{\partial}{\partial x}\right]\left[u - \frac{\phi}{\bar{c}}\right] = 0, \tag{3.6}$$

we see that there are two solutions with characteristic velocities $\bar{u} + \bar{c}$ and $\bar{u} - \bar{c}$. For well-posedness, we must impose one field value at $x = 0$ and one field value at $x = L$ when $\bar{c} > \bar{u}$. When $\bar{c} < |\bar{u}|$ we must impose two field values at the inflow boundary and none at the outflow boundary; see, for example, Elvius (1977).

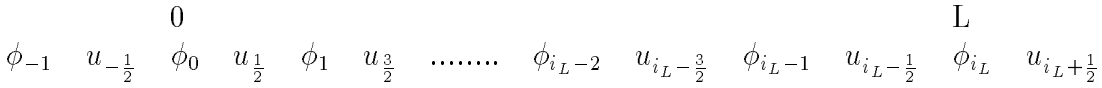

FIGURE 3.1 Distribution of variables on the x-axis using the 'C-grid'.

Let us now perform a two time level SLSI discretization on Eqs. (3.1) and (3.2) using 'C-grid' staggering of the fields (see figure 3.1) ;

$$\phi_i^{n+1} + \frac{\bar{\phi}\Delta t}{2\Delta x}\left(u_{i+\frac{1}{2}}^{n+1} - u_{i-\frac{1}{2}}^{n+1}\right) = R_i^{\phi} = (X^{\phi})_*^n, \tag{3.7}$$

$$u_{i+\frac{1}{2}}^{n+1} + \frac{\Delta t}{2\Delta x}\left(\phi_{i+1}^{n+1} - \phi_i^{n+1}\right) = R_{i+\frac{1}{2}}^{u} = (X^{u})_*^n, \tag{3.8}$$

where

$$(X^{\phi})_i^n = \phi_i^n - \frac{\bar{\phi}\Delta t}{2\Delta x}\left(u_{i+\frac{1}{2}}^n - u_{i-\frac{1}{2}}^n\right) \tag{3.9}$$

$$(X^{u})_{i+\frac{1}{2}}^n = u_{i+\frac{1}{2}}^n - \frac{\Delta t}{2\Delta x}\left(\phi_{i+1}^n - \phi_i^n\right) \tag{3.10}$$

Having computed R^{ϕ} and R^{u}, Eq. (3.8) is substituted in Eq. (3.7) resulting in

$$\phi_i^{n+1} + \bar{\phi}\left(\frac{\Delta t}{2\Delta x}\right)^2\left(\phi_{i+1} - 2\phi_i + \phi_{i-1}\right)^{n+1} = R_i^{\phi} - \frac{\bar{\phi}\Delta t}{2\Delta x}\left(R_{i+\frac{1}{2}}^{u} - R_{i-\frac{1}{2}}^{u}\right) \tag{3.11}$$

Having solved this equation for ϕ with appropriate boundary conditions, $u_{i+\frac{1}{2}}^{n+1}$ can be computed from Eq. (3.8).

3.1 The semi-implicit scheme.

Let us consider a few obvious choices of well-posed boundaries. We postpone until later the discussion of how to compute R^{u} and R^{ϕ} near the boundary. For now we assume that we know how to do it.

3.1.1 Well-posed boundaries for $\bar{c} > \bar{u}$.

When $\bar{c} > \bar{u}$ we must impose one field on each boundary.

Alternative 1. If we choose to impose our boundary values on ϕ_0 and ϕ_{i_L}, the grid points at which each of the equations is valid are shown in table 1, and the solution proceeds elegantly; the boundary conditions fit naturally into Eq. (3.11).

Boundary	Eq. (3.7)	Eq. (3.8)	Eq. (3.9)	Eq. (3.10)	Eq. (3.11)
ϕ_0, ϕ_{i_L}	$1 \rightarrow i_L - 1$	$0 \rightarrow i_L - 1$	$1 \rightarrow i_L - 1$	$0 \rightarrow i_L - 1$	$1 \rightarrow i_L - 1$
p_0, q_{i_L}	$0 \rightarrow i_L$	$0 \rightarrow i_L - 1$	$0 \rightarrow i_L$	$0 \rightarrow i_L - 1$	$1 \rightarrow i_L - 1$
$u_{\frac{1}{2}}, u_{i_L+\frac{1}{2}}$	$1 \rightarrow i_L$	$1 \rightarrow i_L - 1$	$1 \rightarrow i_L$	$1 \rightarrow i_L - 1$	$2 \rightarrow i_L - 1$
$p_{\frac{1}{2}}, q_{i_L+\frac{1}{2}}$	$1 \rightarrow i_L$	$0 \rightarrow i_L$	$1 \rightarrow i_L$	$0 \rightarrow i_L$	$2 \rightarrow i_L - 1$

TABLE 1. Range of validity of equations (3.7) - (3.11).

Alternative 2. If we choose to impose our boundary values on the fields corresponding to the in-going characteristics valid at the ϕ-points, that is, $p_0 = \phi_0 + \bar{c}u_0$ and $q_{i_L} = \phi_{i_L} - \bar{c}u_{i_L}$, how can we proceed? Let us assume that ϕ_0 and ϕ_{i_L} satisfy Eqs. (3.7), and (3.9) and use the boundary condition to eliminate $u_{-\frac{1}{2}}$ and $u_{i_L+\frac{1}{2}}$:

$$u_{-\frac{1}{2}} = \frac{2}{\bar{c}}(p_0 - \phi_0) - u_{\frac{1}{2}} \qquad u_{i_L+\frac{1}{2}} = \frac{2}{\bar{c}}(\phi_{i_L} - q_{i_L}) - u_{i_L-\frac{1}{2}} \tag{3.12}$$

Then the system of equations (3.11) is closed with the following equations for ϕ_0 and ϕ_{i_L}

$$\left(1 + \frac{\bar{\phi}\Delta t}{\bar{c}\Delta x} + \bar{\phi}\frac{\Delta t^2}{2\Delta x^2}\right)\phi_0^{n+1} - \bar{\phi}\frac{\Delta t^2}{2\Delta x^2}\phi_1^{n+1} = R_0^{\phi} - \bar{\phi}\frac{\Delta t}{\Delta x}\left(R_{\frac{1}{2}}^{u} - \frac{p_0^{n+1}}{\bar{c}}\right) \tag{3.13}$$

$$\left(1 + \frac{\bar{\phi}\Delta t}{\bar{c}\Delta x} + \bar{\phi}\frac{\Delta t^2}{2\Delta x^2}\right)\phi_{i_L}^{n+1} - \bar{\phi}\frac{\Delta t^2}{2\Delta x^2}\phi_{i_L-1}^{n+1} = R_{i_L}^{\phi} + \bar{\phi}\frac{\Delta t}{\Delta x}\left(\frac{q_{i_L}^{n+1}}{\bar{c}} + R_{i_L-\frac{1}{2}}^{u}\right) \tag{3.14}$$

Alternative 3. If we choose to impose our boundary values on $u_{\frac{1}{2}}$ and $u_{i_L+\frac{1}{2}}$ the grid points at which each of the equations is valid are shown in table 1. The system of equations (3.11) is now closed with the following equations for ϕ_1 and ϕ_{i_L}:

$$\phi_1^{n+1} - \bar{\phi}\left(\frac{\Delta t}{2\Delta x}\right)^2\left(\phi_2 - \phi_1\right)^{n+1} = R_1^{\phi} - \bar{\phi}\frac{\Delta t}{2\Delta x}\left(R_{\frac{3}{2}}^{u} - u_{\frac{1}{2}}^{n+1}\right) \tag{3.15}$$

$$\phi_{i_L}^{n+1} - \bar{\phi}\left(\frac{\Delta t}{2\Delta x}\right)^2\left(-\phi_{i_L} + \phi_{i_L-1}\right)^{n+1} = R_{i_L}^{\phi} - \bar{\phi}\frac{\Delta t}{2\Delta x}\left(u_{i_L+\frac{1}{2}}^{n+1} - R_{i_L-\frac{1}{2}}^{u}\right) \tag{3.16}$$

Equation (3.15) results from substituting Eq. (3.8) into Eq. (3.7) with $i = 1$. Equation (3.16) results from substituting Eq. (3.8) with $i = i_L - 1$ into Eq. (3.7) with $i = i_L$.

Alternative 4. If we choose to impose our boundary values on the fields corresponding to the in-going characteristics at the u-points, that is, $p_{\frac{1}{2}} = \phi_{\frac{1}{2}} + \bar{c}u_{\frac{1}{2}}$ and $q_{i_L+\frac{1}{2}} =$

$\phi_{i_L+\frac{1}{2}} - \bar{c}u_{i_L+\frac{1}{2}}$, how can we proceed? Let us now assume that $u_{\frac{1}{2}}$ and $u_{i_L+\frac{1}{2}}$ satisfy Eqs. (3.8), and (3.10) and use the boundary condition to eliminate ϕ_0 and ϕ_{i_L+1}:

$$\phi_0 = 2(p_{\frac{1}{2}} - \bar{c}u_{\frac{1}{2}}) - \phi_1; \qquad \phi_{i_L+1} = 2(q_{i_L+\frac{1}{2}} + \bar{c}u_{i_L+\frac{1}{2}}) - \phi_{i_L} \tag{3.17}$$

Then the system of equations (3.11) is closed with the following equations for ϕ_1 and ϕ_{i_L}

$$\phi_1^{n+1} - \bar{\phi}\Big(\frac{\Delta t}{2\Delta x}\Big)^2\Big(\phi_2 - (1+2\tau)\phi_1\Big)^{n+1} = R_1^\phi - \bar{\phi}\frac{\Delta t}{2\Delta x}\Big(R^u_{\frac{3}{2}} - \tau(R^u_{\frac{1}{2}} + \frac{\Delta t}{\Delta x}p^{n+1}_{\frac{1}{2}})\Big) \tag{3.18}$$

$$\phi_{i_L}^{n+1} - \bar{\phi}\Big(\frac{\Delta t}{2\Delta x}\Big)^2\Big(-(1+2\tau)\phi_{i_L} + \phi_{i_L-1}\Big)^{n+1} = R^\phi_{i_L} - \bar{\phi}\frac{\Delta t}{2\Delta x}\Big(\tau(R^u_{i_L+\frac{1}{2}} - \frac{\Delta t}{\Delta x}q^{n+1}_{L+\frac{1}{2}}) - R^u_{i_L-\frac{1}{2}}\Big) \tag{3.19}$$

where $\tau = 1/(1+\bar{c}\Delta t/\Delta x)$.

Other combinations of u and ϕ can also be used as well-posed boundary conditions. To impose them proceed as above: examine their impact on the u and ϕ equations closest to the boundary and use the resulting ϕ equation to close the system of equations (3.11). The important point is that the boundary conditions and the interior system of equations form a complete system. There is danger of overlooking this point if one is using an imported super-efficient and therefore highly attractive solver. We have done so with the HIRLAM model where we arbitrarily set the second order time difference of the horizontal divergence to zero on the boundary. Because this is a reasonable assumption for meteorological waves, and because the boundary relaxation scheme is very good at damping noise this is a legitimate approximation in the present set-up. For well-posed systems such latitude is not allowed.

3.1.2 Well-posed boundaries for $\bar{c} < |\bar{u}|$.

Now we must impose two fields at the inflow boundary and none at the outflow boundary.

Alternative 1. Impose the boundary values on ϕ and u at the ϕ-points. Assume $\bar{u} > 0$. Then we impose ϕ_0 and u_0, using the latter to compute $u_{-\frac{1}{2}} = 2u_0 - u_{\frac{1}{2}}$. Since we cannot impose ϕ_{i_L} we must design a method of computing it. We cannot naively use Eq. (3.7) since $u_{i_L+\frac{1}{2}}$ is outside the area. Let us try the simplest possible extrapolation for $\partial u/\partial x$ therefore:

$$\phi_{i_L}^{n+1} + \frac{\bar{\phi}\Delta t}{2\Delta x}\Big(u^{n+1}_{i_L-\frac{1}{2}} - u^{n+1}_{i_L-\frac{3}{2}}\Big) = R^\phi_{i_L}. \tag{3.20}$$

For $\bar{u} < 0$ we use the same arguments to arrive at

$$\phi_0^{n+1} + \frac{\bar{\phi}\Delta t}{2\Delta x}\Big(u^{n+1}_{\frac{3}{2}} - u^{n+1}_{\frac{1}{2}}\Big) = R^\phi_0. \tag{3.21}$$

We discuss in section 3.2 the computation of $R^\phi_{i_L}$ and R^ϕ_0 . The system of equations (3.11) is now closed for $\bar{u} > 0$ with the imposed value ϕ_0^{n+1} in conjunction with

$$\phi_{i_L}^{n+1} - \phi_{i_L-1}^{n+1} = R^\phi_{i_L} - R^\phi_{i_L-1}. \tag{3.22}$$

For $\bar{u} < 0$, it is closed with the imposed value $\phi_{i_L}^{n+1}$ in conjunction with

$$\phi_1^{n+1} - \phi_0^{n+1} = R_1^\phi - R_0^\phi. \tag{3.23}$$

Alternative 2. Impose the boundary values at the ϕ-points on the fields corresponding to the characteristics, that is, p_0 and q_0, when $\bar{u} > 0$. Since $\phi_0 = \frac{1}{2}(p_0 + q_0)$ and $u_{-\frac{1}{2}} = (p_0 - q_0)/\bar{c} - u_{\frac{1}{2}}$ the situation is identical to *alternative 1* and the procedure is exactly as outlined there.

Obviously, as in section 3.1.1 other combinations of u and ϕ can be imposed.

3.2 The semi-Lagrangian scheme.

How can we compute R^ϕ and R^u next to the inflow boundary? For example, if we are imposing ϕ on the boundary and $\bar{u} > 0$ how can we compute $R^u_{\frac{1}{2}}$? Even for $|\alpha| < 1$ we need to know

$$(X^u)^n_{-\frac{1}{2}} = u^n_{-\frac{1}{2}} - \frac{\Delta t}{2\Delta x}\left(\phi_0^n - \phi_{-1}^n\right)$$

in order to do so. That is, two fields from outside the boundary are required. In this section we consider various options for attacking this problem.

3.2.1 Trajectory truncation

3.2.1a $\bar{c} > \bar{u}$.

If the departure point is such that the interpolation requires fields outside the area of integration then the trajectory is truncated at the nearest point to the boundary which allows the computation of X without requiring fields extraneous to the integration area. This means the following for the four alternative boundary choices listed in section 3.1.1.

Alternative 1: $R^u = (X^u)^n_{\frac{1}{2}}$ when $x_* < \Delta x/2$; $R^u = (X^u)^n_{i_L-\frac{1}{2}}$ when $x_* > L - \Delta x/2$. $R^\phi = (X^\phi)^n_1$ when $x_* < \Delta x$; $R^\phi = (X^\phi)^n_{i_L-1}$ when $x_* > L - \Delta x$.

Alternative 2: $R^u = (X^u)^n_{\frac{1}{2}}$ when $x_* < \Delta x/2$; $R^u = (X^u)^n_{i_L-\frac{1}{2}}$ when $x_* > L - \Delta x/2$. $R^\phi = (X^\phi)^n_0$ when $x_* < 0$; $R^\phi = (X^\phi)^n_{i_L}$ when $x_* > L$.

Alternative 3: $R^u = (X^u)^n_{\frac{3}{2}}$ when $x_* < 3\Delta x/2$; $R^u = (X^u)^n_{i_L-\frac{1}{2}}$ when $x_* > L - \Delta x/2$. $R^\phi = (X^\phi)^n_1$ when $x_* < \Delta x$; $R^\phi = (X^\phi)^n_{i_L}$ when $x_* > L$.

Alternative 4: $R^u = (X^u)^n_{\frac{1}{2}}$ when $x_* < \Delta x/2$; $R^u = (X^u)^n_{i_L+\frac{1}{2}}$ when $x_* > L + \Delta x/2$. $R^\phi = (X^\phi)^n_1$ when $x_* < \Delta x$; $R^\phi = (X^\phi)^n_{i_L}$ when $x_* > L$.

3.2.1b $\quad \bar{c} < |\bar{u}|$.

Again we are faced with the question: how do we compute R^ϕ and R^u, not just at the inflow boundary, but also at the outflow boundary when $|\alpha| < 1$?

Consider the outflow boundary first. When $|\alpha| < 1$ we need to know $X^\phi_{i_L}$ in order to compute $R^\phi_{i_L}$ in Eq. (3.20), and X^ϕ_0 in order to compute R^ϕ_0 in Eq. (3.21). For consistency with Eqs. (3.20) and (3.21) let us use the same extrapolation for $\partial u/\partial x$:

$$X^\phi_{i_L} = \phi^n_{i_L} - \frac{\bar{\phi}\Delta t}{2\Delta x}\left(u^n_{i_L-\frac{1}{2}} - u^n_{i_L-\frac{3}{2}}\right) \tag{3.24}$$

$$X^\phi_0 = \phi^n_0 - \frac{\bar{\phi}\Delta t}{2\Delta x}\left(u^n_{\frac{3}{2}} - u^n_{\frac{1}{2}}\right) \tag{3.25}$$

Next, consider the inflow boundary. I first tried truncating as described under *alternative 1* in section 3.2.1a. Experiments like those described in section 3.3.2 showed these choices to be ill-posed. That is, when $\bar{u} > 0$ truncating by using $R^u = X^u_{\frac{1}{2}}$ is unstable. Additional testing showed that we must devise an approximation for $X^u_{-\frac{1}{2}}$ so that we can truncate using it. The following simple extrapolation for $\partial\phi/\partial x$ proved to be stable (see section 3.3.2). For $\bar{u} > 0$:

$$(X^u)^n_{-\frac{1}{2}} = 2u_0 - u^n_{\frac{1}{2}} - \frac{\Delta t}{2\Delta x}\left(\phi^n_1 - \phi^n_0\right) \tag{3.26}$$

and for $\bar{u} < 0$:

$$(X^u)^n_{i_L+\frac{1}{2}} = 2u_{i_L} - u^n_{i_L-\frac{1}{2}} - \frac{\Delta t}{2\Delta x}\left(\phi^n_{i_L} - \phi^n_{i_L-1}\right) \tag{3.27}$$

Therefore the trajectories are truncated as follows for *alternatives* (1) and (2) of section 3.1.2:

$R^u = (X^u)^n_{-\frac{1}{2}}$ when $x_* < -\Delta x/2$; $R^u = (X^u)^n_{i_L+\frac{1}{2}}$ when $x_* > L + \Delta x/2$. $R^\phi = (X^\phi)^n_0$ when $x_* < 0$; $R^\phi = (X^\phi)^n_{i_L}$ when $x_* > L$.

3.2.2 **Time interpolation.**

What complications are caused by adding adjustment to the advection equation as far as the time interpolation scheme is concerned? To answer this repeat the arguments of section 2, and discretise Eq. (3.1) as

$$\frac{\phi(x_i, t+\delta t) - \phi(x_i - \bar{u}\delta t, t)}{\delta t} + \frac{\bar{\phi}}{2}\left\{\frac{\partial u}{\partial x}(x_i, t+\delta t) + \frac{\partial u}{\partial x}(x_i - \bar{u}\delta t, t)\right\} = 0, \tag{3.28}$$

which becomes

$$\left\{\phi + \frac{\mu}{\alpha}\frac{\bar{\phi}\Delta t}{2}\frac{\partial u}{\partial x}\right\}^{n+1}_{b+\mu} = \left\{\phi - \frac{\mu}{\alpha}\frac{\bar{\phi}\Delta t}{2}\frac{\partial u}{\partial x}\right\}^{n+1-\frac{\mu}{\alpha}}_{b} \equiv \left\{\hat{X}^\phi(\frac{\mu}{\alpha})\right\}^{n+1-\frac{\mu}{\alpha}}_{b} \tag{3.29}$$

The same arguments lead to the following discretization for Eq. (3.2)

$$\left\{u+\frac{\nu}{\alpha}\frac{\Delta t}{2}\frac{\partial\phi}{\partial x}\right\}_{b+\nu}^{n+1}=\left\{u-\frac{\nu}{\alpha}\frac{\Delta t}{2}\frac{\partial\phi}{\partial x}\right\}_{b}^{n+1-\frac{\nu}{\alpha}}\equiv\left\{\hat{X}^u(\frac{\nu}{\alpha})\right\}_{b}^{n+1-\frac{\nu}{\alpha}} \tag{3.30}$$

Here b represents a boundary line, and μ is the integer number of points the ϕ-point of interest is from the boundary. Also, ν is a half odd-integer which measures the distance the u-point of interest is from the boundary.

Assume $\bar{c}>\bar{u}$. Then well-posedness implies that we impose only one field on each boundary. This means that most of the fields required to compute $\hat{X}^\phi$ and $\hat{X}^u$ are not known on the boundary, even at time level n. How can we proceed? Let us assume for now that we can devise stable extrapolations in space which enable us to compute $\hat{X}^\phi$ and $\hat{X}^u$ at time level n. Then we have two choices. (i) Use $\hat{X}^n$ and $\hat{X}^{n-1}$ to extrapolate to time $\hat{X}^{n+1-\mu/\alpha}$ ($\hat{X}^{n+1-\nu/\alpha}$). I have not been able to invent a stable method for doing this. (ii) Incorporate the time interpolation into the semi-implicit scheme. That is, use Eq. (2.12) to re-write Eqs. (3.29)-(3.30), resulting in

$$\left\{\phi+\bar{\phi}\frac{\mu\Delta t}{2\alpha}\frac{\partial u}{\partial x}\right\}_{b+\mu}^{n+1}-C_+\left(\frac{\mu}{\alpha}\right)\left\{\phi-\bar{\phi}\frac{\mu\Delta t}{2\alpha}\frac{\partial u}{\partial x}\right\}_{b}^{n+1}=C_0\left(\frac{\mu}{\alpha}\right)\left\{\hat{X}^\phi(\frac{\mu}{\alpha})\right\}_{b}^{n}+C_-\left(\frac{\mu}{\alpha}\right)\left\{\hat{X}^\phi(\frac{\mu}{\alpha})\right\}_{b}^{n-1} \tag{3.31}$$

$$\left\{u+\frac{\nu\Delta t}{2\alpha}\frac{\partial\phi}{\partial x}\right\}_{b+\nu}^{n+1}-C_+\left(\frac{\nu}{\alpha}\right)\left\{u-\frac{\nu\Delta t}{2\alpha}\frac{\partial\phi}{\partial x}\right\}_{b}^{n+1}=C_0\left(\frac{\nu}{\alpha}\right)\left\{\hat{X}^u(\frac{\nu}{\alpha})\right\}_{b}^{n}+C_-\left(\frac{\nu}{\alpha}\right)\left\{\hat{X}^u(\frac{\nu}{\alpha})\right\}_{b}^{n-1} \tag{3.32}$$

Now consider the problem of approximating $u, \partial u/\partial x.$ and $\partial\phi/\partial x$ on the boundary. (In order to make the arguments clear assume we are imposing ϕ on the boundary and that $\bar{c}>\bar{u}$). At x_0 the simplest possible extrapolations give

$$u_0=\frac{3}{2}u_{\frac{1}{2}}-\frac{1}{2}u_{\frac{3}{2}};\quad\left(\frac{\partial u}{\partial x}\right)_0=\frac{1}{\Delta x}\left(u_{\frac{3}{2}}-u_{\frac{1}{2}}\right);\quad\left(\frac{\partial\phi}{\partial x}\right)_0=\frac{1}{\Delta x}\left(\phi_1-\phi_0\right). \tag{3.33}$$

Even with these simplest of assumptions the discretization of Eqs. (3.31) and (3.32) leads to a set of equations which are most unattractive from the point of view of programming efficiency. The complications are as follows. (a) Both the left hand and right hand sides of Eqs. (3.31) and (3.32) can formally differ for each half-integer increment of α. As is shown in the Appendix there are three possible equations for $u_{\frac{1}{2}}$. If we use the next highest order of approximation for u_0 there will be five. (The programming complication being that we need 'IF' statements or their equivalents). (b) The number of floating point operations increases significantly. Compare Eqs. (3.8) and (A.9). (c) Because the semi-Lagrangian and semi-implicit systems have become intertwined we no longer have a tri-diagonal system of equations to solve.

From a computing point of view these drawbacks may not be too serious in a single-processor scalar environment. We would simply pay a possibly moderate computational

price for getting the boundaries right. However, with vector processors in an MPP environment these complications seem very serious. For these reasons it is interesting to consider an alternative which avoids these pitfalls, a 'well posed buffer zone'.

3.2.3 **Well posed buffer zone.**

How can we fill a well-posed buffer zone when some of the needed fields cannot be imposed externally? For discussion purposes assume $\bar{c} > \bar{u}$. Then we must impose only one field on each boundary. Knowing that field at all times can enable us to estimate its value in the buffer zone using the equations of motion. The other field, which to maintain well-posedness we must not impose externally, presents a problem. How can we estimate it stably using only fields from the interior?

Gustafsson et al., (1972) showed that, for the Lax Wendroff scheme, many extrapolations cause instability on $0 \leq x \leq 1; t > 0$. We can infer that such extrapolations will also be unstable for the semi-Lagrangian schemes since the Lax Wendroff scheme corresponds to the latter with quadratic interpolation when $|\alpha| < 1$. A scheme which they proved to be stable uses Eqs. (3.5) or (3.6) to extrapolate the field corresponding to the outgoing characteristic to the boundary. Let us put a semi-Lagrangian twist to this idea.

For $\bar{u} > 0$ at $x = 0$ we extrapolate q_0 from the interior using

$$\frac{\partial q}{\partial t} + (\bar{u} - \bar{c})\frac{\partial q}{\partial x} = 0. \tag{3.34}$$

For $\bar{u} < 0$ at $x = x_{i_L}$ we extrapolate p_{i_L} from the interior using

$$\frac{\partial p}{\partial t} + (\bar{u} + \bar{c})\frac{\partial p}{\partial x} = 0. \tag{3.35}$$

To maintain stability we solve these by finding the value of the field at the departure point $x_{*q} = x_0 - (\bar{u} - \bar{c})\Delta t$ and $x_{*p} = x_{i_L} - (\bar{u} + \bar{c})\Delta t$, respectively:

$$q\{x_0, (n+1)\Delta t\} = q\{x_0 - (\bar{u} - \bar{c})\Delta t, n\Delta t\} \tag{3.36}$$

$$p\{x_{i_L}, (n+1)\Delta t\} = p\{x_{i_L} - (\bar{u} + \bar{c})\Delta t, n\Delta t\} \tag{3.37}$$

Since we now know q^{n+1} at x_0 we can compute $(\partial q/\partial t)^n$ and $(\partial^2 q/\partial t^2)^n$ there; also knowing p^{n+1} at x_{i_L} means we can compute $(\partial p/\partial t)^n$ and $(\partial^2 q/\partial t^2)^n$ there. Thus we can use Eqs. (3.34) and (3.35) to compute $\partial\phi/\partial x$ and $\partial u/\partial x$:

$$\left(\frac{\partial \phi}{\partial x}\right) = -\frac{1}{2}\left(\frac{1}{\bar{u} + \bar{c}}\frac{\partial p}{\partial t} + \frac{1}{\bar{u} - \bar{c}}\frac{\partial q}{\partial t}\right); \tag{3.38}$$

$$\left(\frac{\partial u}{\partial x}\right) = -\frac{1}{2\bar{c}}\left(\frac{1}{\bar{u} + \bar{c}}\frac{\partial p}{\partial t} - \frac{1}{\bar{u} - \bar{c}}\frac{\partial q}{\partial t}\right); \tag{3.39}$$

By the same method,

$$\left(\frac{\partial^2\phi}{\partial x^2}\right) = \frac{1}{2(\bar{u}+\bar{c})^2}\left(\frac{\partial^2 p}{\partial t^2}\right) + \frac{1}{2(\bar{u}-\bar{c})^2}\left(\frac{\partial^2 q}{\partial t^2}\right) \tag{3.40}$$

$$\left(\frac{\partial^2 u}{\partial x^2}\right) = \frac{1}{2\bar{c}(\bar{u}+\bar{c})^2}\left(\frac{\partial^2 p}{\partial t^2}\right) - \frac{1}{2\bar{c}(\bar{u}-\bar{c})^2}\left(\frac{\partial^2 q}{\partial t^2}\right) \tag{3.41}$$

We can now use the Taylor expansion, Eq. (2.15) to estimate ϕ in the buffer zone and the following Taylor expansion can then be used to compute u there:

$$u\{(i-\Delta x/2), n\Delta t\} = \left[u - (i-\Delta x/2)\frac{\partial u}{\partial x} + \frac{(i-\Delta x/2)^2}{2}\frac{\partial^2 u}{\partial x^2} + ...\right]^n \tag{3.42}$$

Alternative 1. If we choose to impose our boundary values on ϕ_0 and ϕ_{i_L}, then we must substitute $p = 2\phi - q$ at x_0 and $q = 2\phi - p$ at x_{i_L} in Eqs. (3.38) - (3.41).

Alternative 2. If we choose to impose our boundary values on the fields corresponding to the in-going characteristics valid at the ϕ-points, that is, $p_0 = \phi_0 + \bar{c}u_0$ and $q_{i_L} = \phi_{i_L} - \bar{c}u_{i_L}$, we can apply Eqs. (3.38) - (3.41) directly.

3.3 Numerical testing.

For our numerical tests let us use a sine wave of wavelength L as an initial state:

$$\phi(x,0) = \hat{\phi}sin\left(\frac{2\pi}{L}x\right); \qquad u(x,0) = \frac{\hat{\phi}}{\bar{c}}sin\left(\frac{2\pi}{L}x\right) \tag{3.43}$$

We will choose our boundary conditions such that this wave moves in the positive x direction with a velocity $\bar{u}+\bar{c}$.

As in section 2, I have chosen $L = 1000km, \Delta x = 10$km. In the tests which follow the length of the integration (T) will always be chosen such that the wave moves *exactly* a distance L. Thus the initial and final state should be identical in the figure showing the solution. This makes any errors 'jump out'. For the same reason, the fields p and q corresponding to the characteristics will be displayed. Again, a solution with a non-zero q, which indicates errors, will 'jump out'.

3.3.1 Trajectory truncation and $\bar{c} > \bar{u}$.

The boundary conditions for $\bar{c} > \bar{u}$ are for *alternatives (1), (2), (3), (4)* of section 3.1.1, respectively:

$$\phi(0,t) = \hat{\phi}sin\left(\frac{2\pi}{L}\{0 - (\bar{u}+\bar{c})t\}\right); \qquad \phi(L,t) = \hat{\phi}sin\left(\frac{2\pi}{L}\{L - (\bar{u}+\bar{c})t\}\right): \tag{3.44}$$

$$p(0,t) = 2\hat{\phi} sin\Big(\frac{2\pi}{L}\{0 - (\bar{u}+\bar{c})t\}\Big); \qquad q(L,t) = 0 : \tag{3.45}$$

$$u(\frac{\Delta x}{2},t) = \frac{\hat{\phi}}{\bar{c}} sin\Big(\frac{2\pi}{L}\{\frac{\Delta x}{2} - (\bar{u}+\bar{c})t\}\Big); \qquad u(L+\frac{\Delta x}{2},t) = \frac{\hat{\phi}}{\bar{c}} sin\Big(\frac{2\pi}{L}\{L+\frac{\Delta x}{2} - (\bar{u}+\bar{c})t\}\Big) : \tag{3.46}$$

$$p(\frac{\Delta x}{2},t) = 2\hat{\phi} sin\Big(\frac{2\pi}{L}\{\frac{\Delta x}{2} - (\bar{u}+\bar{c})t\}\Big); \qquad q(L+\frac{\Delta x}{2},t) = 0. \tag{3.47}$$

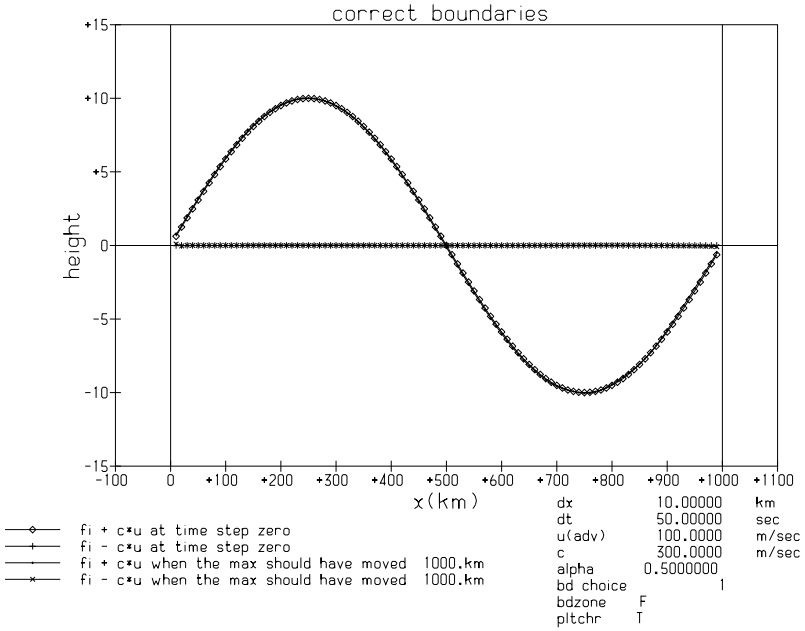

FIGURE 3.2. Graph of the solution of Eqs. (3.1)-(3.2) with initial conditions given by Eqs. (3.43) and ϕ imposed on the boundaries, Eq. (3.44). At time zero p is shown by the diamonds and q by the '+'s. These also represent the analytical solution at time T. The result of integrating with $\Delta t = 50s, \bar{c} = 300m/s, \bar{u} = 100m/s, \alpha = 0.5$ is displayed as dots for p and as 'x's for q.

Do the semi-implicit discretizations described in section 3.1.1 combined with trajectory truncation as described in section 3.2.1a constitute a well-posed system for $|\alpha| < 1$? For this test $\Delta t = 50s, \bar{c} = 300m/s, \bar{u} = 100m/s, \alpha = 0.5$. All four boundary conditions give stable and accurate forecasts, with nothing to choose between them. In figure 3.2 is displayed the forecast when ϕ is imposed on the boundaries (*alternative 1* in section 3.1.1). Notice that the solution $p(x,T)$ almost exactly overlaps $p(x,0)$, and that the solution $q(x,T)$ equals zero. The integrations corresponding to the three other boundary choices are not displayed but they are equally accurate.

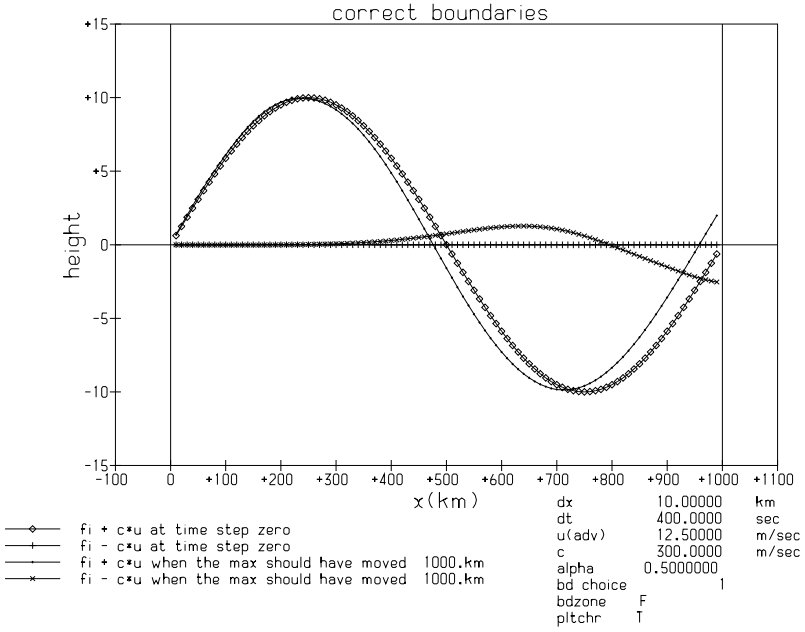

FIGURE 3.3. Same as figure 3.2, but now the result of integrating with $\Delta t = 400s, \bar{u} = 12.5m/s, \alpha = 0.5$ *is displayed as dots for* p *and as 'x's for* q*.*

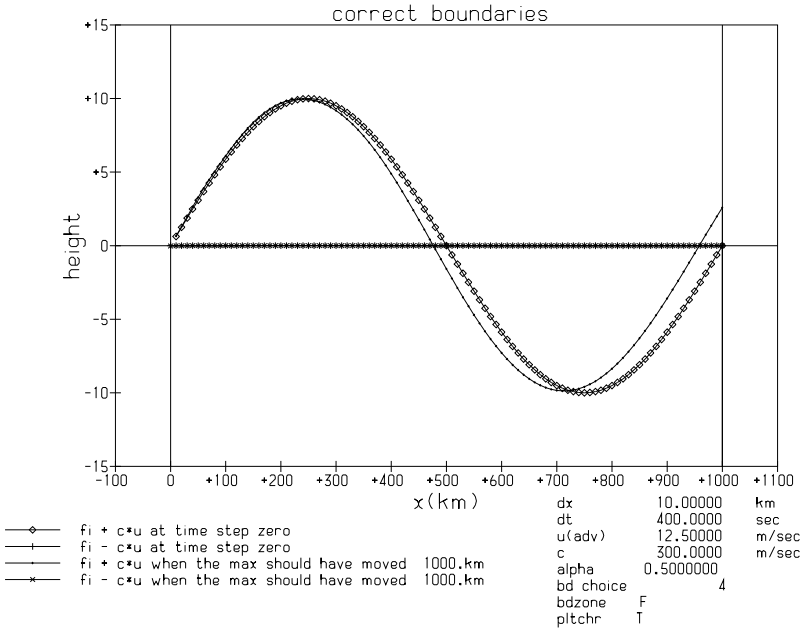

FIGURE 3.4. Graph of the solution of Eqs. (3.1)-(3.2) with initial conditions given by Eqs. (3.43) and p *and* q *imposed on the boundaries, Eq. (3.45). At time zero* p *is shown by the diamonds and* q *by the '+'s. These also represent the analytical solution at time* T*. The result of integrating with* $\Delta t = 400s, \bar{c} = 300m/s, \bar{u} = 12.5m/s, \alpha = 0.5$ *is displayed as dots for* p *and as 'x's for* q*.*

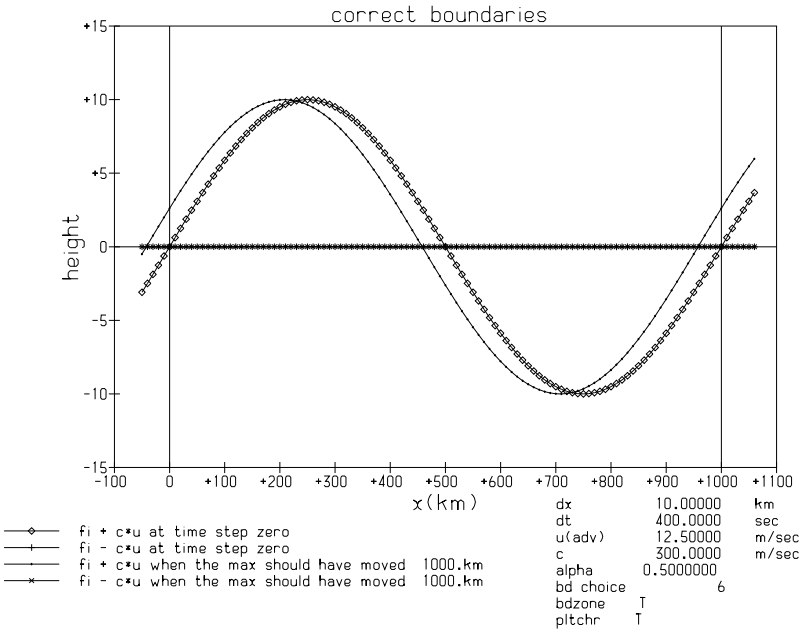

FIGURE 3.5. Graph of the solution of Eqs. (3.1)-(3.2) with initial conditions given by Eqs. (3.43) and cyclic boundaries. At time zero p is shown by the diamonds and q by the '+'s. These also represent the analytical solution at time T. The result of integrating with $\Delta t = 400s, \bar{c} = 300m/s, \bar{u} = 12.5m/s, \alpha = 0.5$ *is displayed as dots for p and as 'x's for q.*

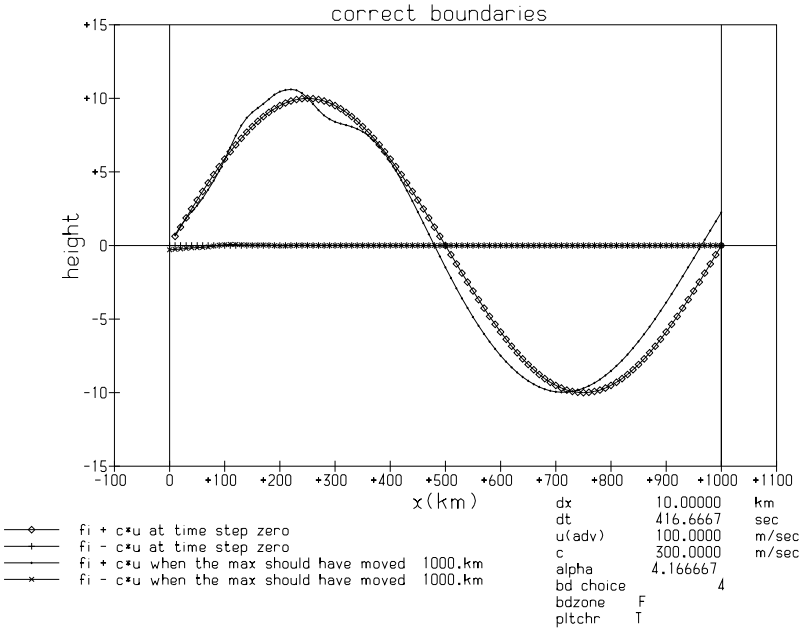

FIGURE 3.6. Same as figure 3.4, but now the result of integrating with $\Delta t = 400s, \bar{u} = 100m/s, \alpha = 4.1667$ *is displayed as dots for p and as 'x's for q.*

If the time step is large enough to cause a discrepancy between the analytic and discretized solution is the system still well-posed? This corresponds somewhat to the meteorological situation where gravity waves are modelled inaccurately. For this test $\Delta t = 400s, \bar{c} = 300m/s, \bar{u} = 12.5m/s, \alpha = 0.5$. All four boundary conditions give stable but slightly inaccurate forecasts. In figure 3.3 is displayed the forecast when ϕ is imposed on the boundaries (*alternative 1* in section 3.1.1). Notice that the solution $p(x,T)$ has a time truncation error. Also, notice that the solution $q(x,T)$ is non-zero. The latter can be remedied by imposing p_0 and q_{i_L} on the boundaries; (*alternative 2* in section 3.1.1). The result is shown in figure 3.4. Now, $p(x,T)$ is as accurate as in figure 3.3, but $q(x,T)$ is zero, as it should be. Imposing u on the boundaries at the u-points (*alternative 3* in section 3.1.1) also gives a forecast with non-zero $q(x,T)$; imposing $p_{\frac{1}{2}}$ and $q_{i_L+\frac{1}{2}}$ (*alternative 4* in section 3.1.1) has $q(x,T) = 0$. We will postpone a discussion of whether there is a 'best choice' of well-posed boundary condition until we try to implement the ideas of Engquist and Majda (1977) but obviously *alternatives* (2) and (4) are superior to *alternatives* (1) and (3) because they prevent the other gravity wave from being excited. For comparison the forecast for cyclic boundary conditions is displayed in figure 3.5. Notice the slowing down of the wave caused by the time truncation error.

Let us now put a severe strain on our trajectory truncation scheme by increasing α to 4.1667. For this test $\Delta t = 400s, \bar{c} = 300m/s, \bar{u} = 100m/s, \alpha = 4.1667$. Let us impose p_0 and q_{i_L} on the boundaries (*alternative 2* in section 3.1.1). The result can be seen in figure 3.6. The good news is that trajectory truncation is stable even when the departure point is over four grid points outside the integration area. The not so good news is that an additional error has been generated, as can be seen by comparing figures 3.6 and 3.4. The other three boundary options discussed in section 3.1.1 give almost identical results for $p(x,T)$.

3.3.2 Trajectory truncation and $\bar{c} < |\bar{u}|$.

The boundary conditions now become for *alternative 1* with $\bar{u} > 0$

$$\phi(0,t) = \hat{\phi} sin\Big(\frac{2\pi}{L}\{0 - (\bar{u}+\bar{c})t\}\Big); \qquad u(0,t) = \frac{\phi(0,t)}{\bar{c}}, \tag{3.48}$$

and for *alternative 1* with $\bar{u} < 0$

$$\phi(L,t) = \hat{\phi} sin\Big(\frac{2\pi}{L}\{L - (\bar{u}+\bar{c})t\}\Big); \qquad u(L,t) = \frac{\phi(L,t)}{\bar{c}}, \tag{3.49}$$

For *alternative 2* with $\bar{u} > 0$

$$p(0,t) = 2\hat{\phi} sin\Big(\frac{2\pi}{L}\{0 - (\bar{u}+\bar{c})t\}\Big); \qquad q(0,t) = 0 :, \tag{3.50}$$

and for *alternative 2* with $\bar{u} < 0$

$$p(L,t) = 2\hat{\phi} sin\Big(\frac{2\pi}{L}\{L - (\bar{u}+\bar{c})t\}\Big); \qquad q(L,t) = 0 :, \tag{3.51}$$

Do the semi-implicit discretizations described in section 3.1.2 combined with trajectory truncation (*option 1* in section 3.2.1b) constitute a well-posed system for $|\alpha| < 1$? For this test $\Delta t = 100s, \bar{c} = 30m/s, \bar{u} = 50m/s, \alpha = 0.5$. Both boundary alternatives give stable and accurate forecasts, with nothing to choose between them (I have not displayed them as they are indistinguishable from figure 3.2). The important lesson is that the extrapolations forced on us by the complications at both inflow and outflow are stable and accurate.

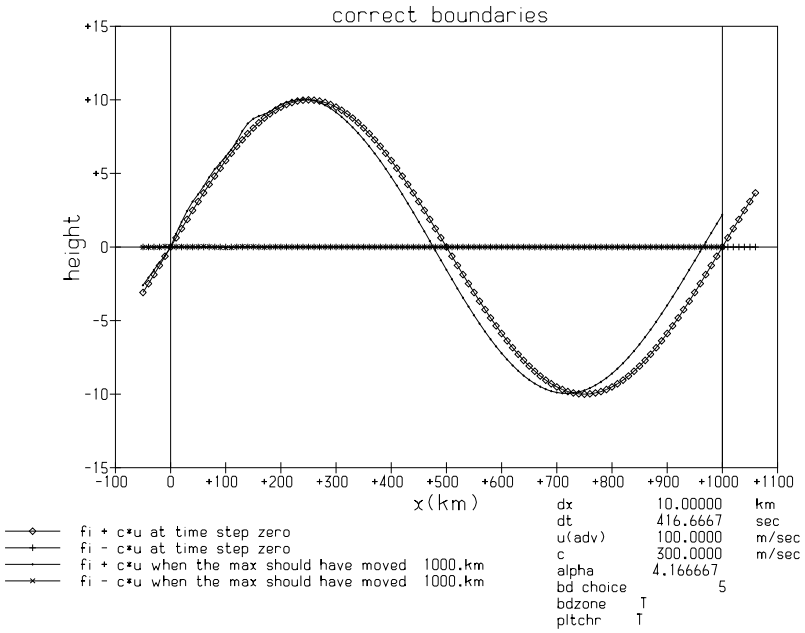

FIGURE 3.7. Same as figure 3.6, but now replacing trajectory truncation with the well posed buffer zone.

3.3.3 **Well posed buffer zone and $\bar{c} > \bar{u}$.**

The boundary conditions for *alternative 1* are given by Eq. (3.44) and for *alternative 2* by Eq. (3.45).

Is the well-posed buffer zone constructed in section 3.2.3 stable? Does it offer any advantage over trajectory truncation? To answer, the large α test was repeated, but now using the well-posed buffer zone. Thus, $\Delta t = 400s, \bar{c} = 300m/s, \bar{u} = 100m/s, \alpha = 4.1667$. With p_0 and q_{i_L} imposed on the boundaries the result is shown in figure 3.7. As can be seen the forecast is stable, and comparing it with figure 3.6 it is also more accurate. (Imposing ϕ on the boundaries gives an equally accurate forecast for p and, as previously, a non-zero q.

4. **DISCUSSION.**

We have concentrated on practical details in this note. They raise the obvious theoretical question: can we prove stability for the discretized systems we have examined? For the one dimensional advection equation trajectory truncation is stable in the von Neumann sense. (See Eqs. (21)-(24) of McDonald (1984). The amplification factor is equal to one when $\hat{\alpha} = 0$.) However, this does not guarantee stability of the initial boundary value system. One may speculate that the time interpolation scheme is stable; see Skålin and Lie (1995). As far as the well-posed buffer zone is concerned, Gustafsson, Kreiss, and Sundström (1972) have given a proof of stability for this initial boundary value problem for $|\alpha| \leq 1$ and quadratic interpolation. Their approach offers us a template for proving stability for all of these schemes. We hope to address this issue in a future note.

As we have seen, inventing well-posed boundaries even for simple one-dimensional systems is a non-trivial task. When we move to two dimensions the complications multiply, principally because the characteristics need not impinge normally on the boundary. Nevertheless, Engquist and Majda (1977) have established a method for constructing boundary conditions which are well-posed and perfectly transparent at normal incidence. At other angles of incidence (except tangential) reflections at the boundary can be reduced to a minimum by their method. The plan is to use their ideas and those discussed in this note to construct a two-dimensional SLSI shallow water model with 'transparent boundaries'. We intend to describe our experiences in a future note.

It would be nice to invent a less cumbersome implementation of the time interpolation idea than that outlined in the appendix. Similarly, the question arises: is there another way of building a well posed buffer zone? Gustafsson, Kreiss, and Sundström (1972) discuss other methods for Eulerian schemes. Can we invent equivalent schemes which are stable for $|\alpha| > 1$?

Finally, although we have concentrated on looking at well-posed boundaries for semi-Lagrangian schemes in this note, Eulerian systems are equally problematic. Consider an Eulerian approach using fourth order spatial differencing. This will, in principle, require knowledge of fields outside the boundaries. Thus, stable extrapolations will be required to update the fields in the vicinity of the boundary. A possible solution is to adopt the upstream ideas inherent in the semi-Lagrangian approach. See also, however, Elvius and Sundström (1973).

Acknowledgement. Thanks to Nils Gustafsson, Bent Hansen-Sass and Peter Lynch for their critical reading of the manuscript, and to Jim Hamilton for assistance with the graphics.

5. REFERENCES.

Bates, J.R., and A. McDonald, 1982: Multiply-upstream, Semi-Lagrangian advective schemes: analysis and application to a multi-level primitive equation model. *Mon. Wea. Rev.,* **110**, 1831-1842.

Davies, H.C., 1976: A lateral boundary formulation for multi-level prediction models. *Q. J. Roy. Met. Soc.,* **102**, 405-418.

Elvius, T. and A. Sundström, 1973: Computationally efficient schemes and boundary conditions for a fine mesh barotropic model based on the shallow water equations. *Tellus,* **25**, 132-156.

Elvius, T., 1977: Experiments with a primitive equations model for limited area forecasts. *Beitr. Phys. Atmosph.,* **50**, 367-392.

Engquist, B., and A. Majda, 1977: Absorbing boundary conditions for the numerical simulation of waves. *Math. Comput.,* **31**, 629-651.

Falcone, M., and R. Ferretti 1998: Convergence analysis for a class of high-order semi-Lagrangian advection schemes. *SIAM J. Numer. Anal.,* **35** 909-940.

Gustafsson, B., H.-O. Kreiss and A. Sundström, 1972: Stability theory of difference approximations for mixed initial boundary value problems. *Math. Comput.,* **26**, 649-686.

Gustafsson, N., E. Källén, and S. Thorsteinsson 1998: Sensitivity of forecast errors to initial and lateral boundary conditions. *Tellus,* **50A**, 167-185.

McDonald, A., 1984: Accuracy of Multiply-Upstream semi-Lagrangian advective schemes. *Mon. Wea. Rev.,* **112**, 1267-1275.

McDonald, A., 1997: Lateral boundary conditions for operational regional forecast models; a review. *HIRLAM technical report* **32**

McDonald, A., 1998: Conservation of mass in HIRLAM. *HIRLAM newsletter* **32,** 39-44.

Oliger, J. and A. Sundström, 1978: Theoretical and practical aspects of some initial boundary value problems in fluid dynamics. *S.I.A.M. J. Appl. Math.,* **35**, 419-446.

Skålin, R, and I. Lie 1995: On the stability of semi-Lagrangian advection with interpolation in time. *Available from Ivar Lie, DNMI, P.O. Box 43, Blindern, N-0313 OSLO, Norway.*

6. APPENDIX.

In order to give a background for the discussion in section 3.2.2 the equations for $0 < \alpha \leq 1.5$ for the time interpolation scheme are derived. We are approximating Eqs. (3.31) and (3.32) using Eq. (3.33) to estimate the fields on the boundary.

For $0 < \alpha \leq 0.5$ we use trajectory truncation:

$$u_{\frac{1}{2}}^{n+1} + \frac{\Delta t}{2\Delta x}\Big(\phi_1^{n+1} - \phi_0^{n+1}\Big) = (X^u)_{\frac{1}{2}}^{n}. \tag{A.1}$$

For $\alpha > 0.5$ we have

$$\Big[u_{\frac{1}{2}} + \frac{1}{2\alpha}\frac{\Delta t}{2\Delta x}(\phi_1 - \phi_0)\Big]^{n+1} - C_+\Big(\frac{1}{2\alpha}\Big)\Big[1.5u_{\frac{1}{2}} - 0.5u_{\frac{3}{2}} - \frac{1}{2\alpha}\frac{\Delta t}{2\Delta x}(\phi_1 - \phi_0)\Big]^{n+1} = \tilde{R}_{\frac{1}{2}}^{u} \tag{A.2}$$

where

$$\tilde{R}_{\frac{1}{2}}^{u} = C_0\Big(\frac{1}{2\alpha}\Big)\Big[\tilde{X}^u\Big(\frac{1}{2\alpha}\Big)\Big]_0^n + C_-\Big(\frac{1}{2\alpha}\Big)\Big[\tilde{X}^u\Big(\frac{1}{2\alpha}\Big)\Big]_0^{n-1} \tag{A.3}$$

and

$$\tilde{X}^u\Big(\frac{\nu}{\alpha}\Big) = 1.5u_{\frac{1}{2}} - 0.5u_{\frac{3}{2}} - \frac{\nu}{\alpha}\frac{\Delta t}{2\Delta x}(\phi_1 - \phi_0) \tag{A.4}$$

For $0.5 < \alpha \leq 1.5$, $u_{\frac{3}{2}}^{n+1}$ is given by Eq. (3.8), which when substituted in Eq. (A.2) gives

$$\{1 - 1.5C_+\Big(\frac{1}{2\alpha}\Big)\}u_{\frac{1}{2}}^{n+1} +$$

$$\frac{\Delta t}{2\Delta x}\Big[-0.5C_+\Big(\frac{1}{2\alpha}\Big)(\phi_2 - \phi_1) + \frac{1}{2\alpha}\{1 + C_+\Big(\frac{1}{2\alpha}\Big)\}(\phi_1 - \phi_0)\Big]^{n+1} = \tilde{R}_{\frac{1}{2}}^{u} - 0.5C_+\Big(\frac{1}{2\alpha}\Big)R_{\frac{3}{2}}^{u} \tag{A.5}$$

For $\alpha > 1.5$, on the other hand Eq. (3.8) must be replaced by

$$\Big[u_{\frac{3}{2}} + \frac{3}{2\alpha}\frac{\Delta t}{2\Delta x}(\phi_2 - \phi_1)\Big]^{n+1} - C_+\Big(\frac{3}{2\alpha}\Big)\Big[1.5u_{\frac{1}{2}} - 0.5u_{\frac{3}{2}} - \frac{3}{2\alpha}\frac{\Delta t}{2\Delta x}(\phi_1 - \phi_0)\Big]^{n+1} = \tilde{R}_{\frac{3}{2}}^{u}, \tag{A.6}$$

where

$$\tilde{R}_{\frac{3}{2}}^{u} = C_0\Big(\frac{3}{2\alpha}\Big)\Big[\tilde{X}^u\Big(\frac{3}{2\alpha}\Big)\Big]_0^n + C_-\Big(\frac{3}{2\alpha}\Big)\Big[\tilde{X}^u\Big(\frac{3}{2\alpha}\Big)\Big]_0^{n-1}. \tag{A.7}$$

When Eq. (A.6) is substituted in Eq. (A.2) we get

$$\{1 + 0.5C_+\Big(\frac{3}{2\alpha}\Big) - 1.5C_+\Big(\frac{1}{2\alpha}\Big)\}u_{\frac{1}{2}}^{n+1} +$$

$$\Big[\frac{1}{2\alpha}\{1 + C_+\Big(\frac{1}{2\alpha}\Big)\}\{1 + 0.5C_+\Big(\frac{3}{2\alpha}\Big)\} + \frac{3}{4\alpha}C_+\Big(\frac{1}{2\alpha}\Big)C_+\Big(\frac{3}{2\alpha}\Big)\Big]\frac{\Delta t}{2\Delta x}(\phi_1 - \phi_0)^{n+1}$$

$$-\frac{3}{4\alpha}C_+\Big(\frac{1}{2\alpha}\Big)\frac{\Delta t}{2\Delta x}(\phi_2 - \phi_1)^{n+1} = \{1 + 0.5C_+\Big(\frac{3}{2\alpha}\Big)\}\tilde{R}_{\frac{1}{2}}^{u} - 0.5C_+\Big(\frac{1}{2\alpha}\Big)\tilde{R}_{\frac{3}{2}}^{u} \tag{A.8}$$

Similarly, for $\alpha > 1.5$,

$$\{1 + 0.5C_+\Big(\frac{3}{2\alpha}\Big) - 1.5C_+\Big(\frac{1}{2\alpha}\Big)\}u_{\frac{3}{2}}^{n+1} +$$

$$\left[\frac{3}{4\alpha}\{1+C_+\left(\frac{1}{2\alpha}\right)\}C_+\left(\frac{3}{2\alpha}\right)+\frac{3}{2\alpha}\{1-1.5C_+\left(\frac{1}{2\alpha}\right)\}C_+\left(\frac{3}{2\alpha}\right)\right]\frac{\Delta t}{2\Delta x}(\phi_1-\phi_0)^{n+1}$$
$$+\frac{3}{2\alpha}\{1-1.5C_+\left(\frac{1}{2\alpha}\right)\}\frac{\Delta t}{2\Delta x}(\phi_2-\phi_1)^{n+1}=1.5C_+\left(\frac{3}{2\alpha}\right)\tilde{R}^u_{\frac{1}{2}}+\{1-1.5C_+\left(\frac{1}{2\alpha}\right)\}\tilde{R}^u_{\frac{3}{2}} \quad (A.9)$$

If $0<\alpha\leq 1$,

$$\phi_1^{n+1}+\frac{\bar{\phi}\Delta t}{2\Delta x}\left(u_{\frac{3}{2}}^{n+1}-u_{\frac{1}{2}}^{n+1}\right)=R_1^{\phi} \quad (A.10)$$

To derive an equation for ϕ only, corresponding to Eq. (3.11), we do the following. When $0<\alpha\leq 0.5$ we substitute for $u_{\frac{3}{2}}$ from Eq. (3.8) and $u_{\frac{1}{2}}$ from Eq. (A.1). When $0.5<\alpha\leq 1$ we substitute for $u_{\frac{3}{2}}$ from Eq. (3.8) and $u_{\frac{1}{2}}$ from Eq. (A.5). However, for $\alpha>1$, we must use

$$\left[\phi_1+\frac{1}{\alpha}\frac{\Delta t\bar{\phi}}{2\Delta x}(u_{\frac{3}{2}}-u_{\frac{1}{2}})\right]^{n+1}-C_+\left(\frac{1}{\alpha}\right)\left[\phi_0-\frac{1}{\alpha}\frac{\Delta t\bar{\phi}}{2\Delta x}(u_{\frac{3}{2}}-u_{\frac{1}{2}})\right]^{n+1}=\tilde{R}_1^{\phi} \quad (A.11)$$

where

$$\tilde{R}_1^{\phi}=C_0\left(\frac{1}{\alpha}\right)\left[\tilde{X}^{\phi}\left(\frac{1}{\alpha}\right)\right]_0^n+C_-\left(\frac{1}{\alpha}\right)\left[\tilde{X}^{\phi}\left(\frac{1}{\alpha}\right)\right]_0^{n-1} \quad (A.12)$$

and

$$\left[\tilde{X}^{\phi}\left(\frac{\mu}{\alpha}\right)\right]_0=\phi_0-\frac{\mu}{\alpha}\frac{\Delta t\bar{\phi}}{2\Delta x}(u_{\frac{3}{2}}-u_{\frac{1}{2}}) \quad (A.13)$$

When $0.5<\alpha\leq 1.5$ we substitute for $u_{\frac{3}{2}}$ from Eq. (3.8) and $u_{\frac{1}{2}}$ from Eq. (A.1), in Eq. (A.11). When $\alpha>1.5$ we substitute for $u_{\frac{3}{2}}$ from Eq. (A.9) and $u_{\frac{1}{2}}$ from Eq. (A.8), in Eq. (A.11).